Journal of
Experimental
Botany
www.jxb.oxfordjournals.org

**RESEARCH PAPER**

# $C_2$ photosynthesis generates about 3-fold elevated leaf $CO_2$ levels in the $C_3$–$C_4$ intermediate species *Flaveria pubescens*

**Olav Keerberg[1,*], Tiit Pärnik[1], Hiie Ivanova[1], Burgund Bassüner[2] and Hermann Bauwe[3,*]**

[1] Department of Plant Physiology, Institute of Agricultural and Environmental Sciences, Estonian University of Life Sciences, 51014 Tartu, Estonia
[2] Center for Conservation and Sustainable Development, Missouri Botanical Garden, St. Louis, MO 63166-0299, USA
[3] Department of Plant Physiology, University of Rostock, 18051 Rostock, Germany

* To whom correspondence should be addressed. E-mail: hermann.bauwe@uni-rostock.de; olav.keerberg@emu.ee

## Abstract

Formation of a photorespiration-based $CO_2$-concentrating mechanism in $C_3$–$C_4$ intermediate plants is seen as a prerequisite for the evolution of $C_4$ photosynthesis, but it is not known how efficient this mechanism is. Here, using *in vivo* Rubisco carboxylation-to-oxygenation ratios as a proxy to assess relative intraplastidial $CO_2$ levels is suggested. Such ratios were determined for the $C_3$–$C_4$ intermediate species *Flaveria pubescens* compared with the closely related $C_3$ plant *F. cronquistii* and the $C_4$ plant *F. trinervia*. To this end, a model was developed to describe the major carbon fluxes and metabolite pools involved in photosynthetic–photorespiratory carbon metabolism and used quantitatively to evaluate the labelling kinetics during short-term $^{14}CO_2$ incorporation. Our data suggest that the photorespiratory $CO_2$ pump elevates the intraplastidial $CO_2$ concentration about 3-fold in leaves of the $C_3$–$C_4$ intermediate species *F. pubescens* relative to the $C_3$ species *F. cronquistii*.

**Key words:** $^{14}CO_2$ labelling, $C_3$–$C_4$ intermediate plants, carbon-concentrating mechanism; *Flaveria*, glycine decarboxylation, photorespiration, photosynthesis.

## Introduction

Land plants form three major classes characterized by specific modes of photosynthetic $CO_2$ assimilation. In $C_3$ plants, $CO_2$ enters metabolism directly via ribulose 1,5-*bis*phosphate (RubP) carboxylase/oxygenase (Rubisco). In the mesophyll of $C_4$ plant leaves and in CAM (crassulacean acid metabolism) plants, $CO_2$ is initially fixed by phosphoenolpyruvate carboxylase. The resulting four-carbon ($C_4$) compounds are decarboxylated in the Rubisco-containing bundle-sheath of $C_4$ plants (Hatch and Slack, 1970) or become stored in the vacuoles of CAM plants for daytime decarboxylation and refixation of the released $CO_2$ by Rubisco (Lüttge, 2004). Both modifications to the $C_3$ mode of $CO_2$ assimilation are adaptations to specific environmental conditions such as low $CO_2$ or water availability. While $C_4$ plants represent only about 3%

of all land plant species, they dominate nearly all grasslands in the tropics, subtropics, and warm temperate zones (Sage, 2004). They also include highly productive crops, such as corn and sugar cane, and there is much interest to introduce yield-relevant features of $C_4$ photosynthesis into $C_3$ crops.

Given the ecological and agricultural significance of $C_4$ plants, it is important to understand how they evolved and what were the crucial steps in this process. A number of studies have shown that the evolution of $C_4$ photosynthesis was not a unique event but occurred at least 66 times during the past 35 million years (Sage, 2004; Sage *et al.*, 2012). Among these plant lineages, the small genus *Flaveria* (Yellowtops) has received particular attention because it includes species with $CO_2$ assimilation modes ranging from $C_3$ via a broad range

---

Abbreviations: CAM, crassulacean acid metabolism; GDC, glycine decarboxylase; RPPC, reductive pentose phosphate cycle (Calvin–Benson cycle); RubP, ribulose 1,5-*bis*phosphate.

of $C_3$–$C_4$ intermediate species to $C_4$ (Powell, 1978; Apel and Maass, 1981; Ku *et al.*, 1983; Bauwe, 1984). Notably, extant *Flaveria* $C_3$–$C_4$ intermediate species represent true evolutionary intermediates between $C_3$ and $C_4$ photosynthesis (Kopriva *et al.*, 1996; McKown *et al.*, 2005). Major physiological features of such plants are low apparent photorespiration (Apel and Maass, 1981; Holaday *et al.*, 1982, 1984) in combination with an enhanced refixation of photorespiratory $CO_2$ (Holbrook *et al.*, 1985; Bauwe *et al.*, 1987) and high glycine accumulation (Holaday and Chollet, 1983, 1984).

Mechanistically, corresponding to the distribution of the photorespiratory enzyme glycine decarboxylase (GDC) in leaves of $C_4$ plants (Ohnishi and Kanai, 1983), these specific characteristics are closely related to a confinement of GDC activity to the leaf bundle sheath (Hylton *et al.*, 1988; Moore *et al.*, 1988). Based on these and other data, it was hypothesized that $C_3$–$C_4$ intermediate species reduce apparent photorespiration by an efficient refixation of photorespired $CO_2$ in the bundle sheath (Monson *et al.*, 1984; Edwards and Ku, 1987; Rawsthorne, 1992). This initial focus on the importance of $CO_2$ refixation was later extended by the hypothesis that the confinement of glycine decarboxylase could result in a concentration of $CO_2$ in the bundle sheath of $C_3$–$C_4$ intermediate plants (von Caemmerer, 1989; Monson and Rawsthorne, 2000). Today, such a mechanism, in which photorespiratory glycine serves as a vehicle to move '$CO_2$' from the mesophyll to the GDC-containing bundle sheath, is seen as a crucial step during the evolution of $C_4$ photosynthesis (Bauwe, 2011; Sage *et al.*, 2012). In other words, the multiple evolution of $C_4$ photosynthesis might have been triggered by and possibly even required the preceding presence of a much simpler $CO_2$ concentration system than the $C_4$ cycle, based on relatively small alterations to the high-flux photorespiratory glycine metabolism.

This hypothesis is now widely accepted and the genetic alterations necessary to restrict photorespiratory GDC activity to the bundle sheath are being unravelled (Wiludda *et al.*, 2012; Schulze *et al.*, 2013). On the other hand, it is not known how efficient this photorespiratory $CO_2$ pump could be. Here, $^{14}CO_2$ incorporation studies designed to obtain an estimate of the *in vivo* rates of the two Rubisco-catalysed reactions in the $C_3$–$C_4$ species *Flaveria pubescens* relative to the control $C_3$ species *Flaveria cronquistii* are reported. The ratio of these reactions, carboxylation versus oxygenation of RuBP, is co-determined by kinetic parameters of Rubisco and by the $CO_2$/$O_2$ concentration ratio (Laing *et al.*, 1974; Peisker, 1974; Farquhar *et al.*, 1980). Hence, a higher *in vivo* carboxylation/oxygenation ratio in *F. pubescens* relative to a control $C_3$ species would not only indicate an elevated $CO_2$/$O_2$ concentration ratio but also allow quantifying the efficiency of the photorespiratory $CO_2$ pump.

## Materials and methods

### Plant growth and $^{14}C$ labelling

*Flaveria cronquistii* A.M. Powell ($C_3$), *Flaveria pubescens* Rydberg ($C_3$–$C_4$), and *Flaveria trinervia* (Spreng.) C. Mohr ($C_4$) were grown in soil in a controlled environment chamber at 28/22 °C (day/night) and 250–300 µmol photons $m^{-2}$ $s^{-1}$ at a photoperiod of 16 h. Fully expanded leaves excised from 40–60-d-old plants were fixed by thin wires in a frame positioned in a purpose-built fast-acting $^{14}CO_2$ labelling device (Pärnik *et al.*, 1987). Leaves were pre-illuminated at 30 Pa $^{12}CO_2$ and 210 kPa $O_2$ for 10–15 min at about 1200 µmol photons $m^{-2}$ $s^{-1}$ and 25 °C to ensure maximum stomata opening and achievement of the steady-state rate of photosynthesis. Plants were then exposed to $^{14}CO_2$ (2000 MBq $mmol^{-1}$) for 0.6, 1.2, 2.4, 5, 15, 60, 120, and 360 s at the same concentrations of $CO_2$ and $O_2$, temperature and light as applied during pre-illumination. At the given time points, within 0.1 s, the leaf samples were automatically transferred into boiling 80% ethanol. $^{14}CO_2$ incorporation was linear over the whole experiment. All experiments were performed in triplicate (three individual plants in three consecutive days, resulting in three leaf samples per time-point for each species).

### Metabolite analysis

All leaf samples were individually extracted as described before (Värk *et al.*, 1968) with slight modifications. After 2 min in boiling 80% ethanol, the samples were extracted for 15 min at 86 °C with 5 ml of 80% ethanol (twice) and 20% ethanol (once). All four ethanolic fractions were combined. The remaining samples were then further extracted for 15 min at 86 °C with 5 ml 96% ethanol acidified with 3 drops of 3 N HCl. The two extracts were separately (to avoid the hydrolysis of disaccharides) dried at 37 °C, individually re-dissolved in 5 ml $H_2O$ each and cleared by centrifugation. The supernatants were combined, dried as above, and the metabolites re-dissolved in 1 ml $H_2O$. This final extract was used to determine total extractable radioactivity, radioactivity in amino acids (AAA 339 analyzer, Mikrotechna, Czech Republic), and other metabolites by using two-dimensional paper chromatography. Residual radioactivity in the fully extracted, dried, and triturated leaf samples was determined by using a non-aqueous scintillation cocktail. These analytical methods including the protocol used for starch analysis were described in more detail elsewhere (Keerberg *et al.*, 2011).
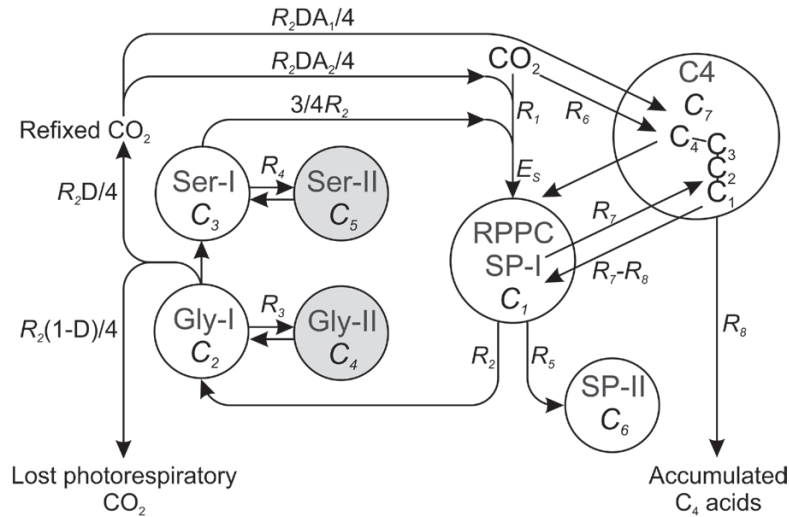
### Photosynthetic–photorespiratory gas exchange

Rates of net and true photosynthesis, photorespiratory $CO_2$ evolution from the leaf, intracellular decarboxylation of early photosynthates, and rates of reassimilation of photorespiratory $CO_2$ were determined during steady-state photosynthesis by using standard gas-exchange measurement techniques in combination with a radiogasometric method described before (Pärnik and Keerberg, 1995, 2007). In short, this method is based on the analysis of time curves of $^{14}CO_2$ evolution from labelled photosynthates in leaves previously exposed to $^{14}CO_2$. Photorespiration (210 kPa $O_2$) and day respiration (15 kPa $O_2$) were distinguished by measurement under different $O_2$ concentrations. Re-fixation ratios ($D$) of photorespiratory $CO_2$ were calculated from $^{14}CO_2$ evolution at the very high concentration of 3 kPa $^{12}CO_2$, where re-fixation of $^{14}CO_2$ evolved inside the cell is close to zero, relative to $^{14}CO_2$ evolution at air levels of $^{12}CO_2$.

### Modelling and data analysis

From the radioactivity values for individual metabolites in combination with the specific radioactivity of the $^{14}CO_2$ fed to leaves, the amounts of carbon incorporated at the selected time points were calculated and plotted against the duration of feeding with $^{14}CO_2$. The amounts of carbon fixed in individual compounds were expressed in absolute (µmol C $m^{-2}$) and relative (per cent of total carbon fixed) units. These experimental labelling curves contain the information about rates of all relevant carbon fluxes and corresponding metabolite pool sizes.

To extract this information on *Flaveria* photosynthetic–photorespiratory metabolism, the model shown in Fig. 1 was used. The model allows $CO_2$ incorporation into the reductive pentose

**Fig. 1.** Model of major photosynthetic-photorespiratory carbon fluxes in *Flaveria* including the reductive pentose phosphate cycle (RPPC) with the attached photorespiratory pathway and the $C_4$ photosynthetic pathway. $R_1$, rate of $CO_2$ fixation in RPPC; $R_2$, rate of carbon flux through the glycolate cycle; $R_3$, rate of carbon exchange between different pools of glycine; $R_4$, rate of carbon exchange between different pools of serine; $R_5$, rate of transport of sugar phosphates out of the RPPC; $R_6$, rate of $CO_2$ fixation by the $C_4$ pathway; $R_7$, rate of carbon flux from RPPC into '$C_3$ skeletons' of $C_4$ acids, $R_8$, rate of accumulation of $C_4$ acids; $C_1$, total pool of sugar phosphates in the RPPC; $C_2$, active pool of the glycine branch of the photorespiratory pathway; $C_3$, active pool of the serine branch of the photorespiratory pathway; $C_4$ and $C_5$, corresponding non-photorespiratory metabolite pools; $C_6$, extra-cyclic pool of sugar phosphates; $C_7$, total pool of $C_4$ acids. $D$ (reassimilation coefficient) describes the fraction of refixed relative to total photorespiratory $CO_2$. $A_1$ and $A_2$ are the partition coefficients describing the relative contributions of the RPPC and the $C_4$ pathway to refixation of photorespiratory $CO_2$. Note that Gly-I and Ser-I also include all other metabolites from the respective branches of the photorespiratory pathway. Gly-II and Ser-II represent less mobile (cytosolic, plastidial, vacuolar) pools of these metabolites.

phosphate cycle (RPPC) either directly with rate $R_1$ or via the $C_4$ cycle with rate $R_6$. Total carbon flux through the photorespiratory cycle is denoted $R_2$. $R_5$ is the export rate of phosphorylated sugars into other pathways, for example, sucrose biosynthesis. $R_7$ denotes the rate of carbon efflux from the RPPC to the $C_3$ skeleton of $C_4$ acids, while $R_8$ describes the rate of accumulation of $C_4$-acids. In order to simplify calculations, metabolites were grouped into four pools: (i) pool 'SP' with sugar phosphates plus 3-phosphoglycerate, (ii) pool 'Gly' with metabolites of the two-carbon branch of the photorespiratory cycle, (iii) pool 'Ser' with metabolites of the three-carbon branch of the photorespiratory cycle, and (iv) pool '$C_4$' with malate and aspartate. Each of these four pools comprises two metabolic sub-pools with different labelling kinetics, for example, photorespiratory pools with rapid turnover in peroxisomes and mitochondria (Gly-I and Ser-I with pools $C_2$ and $C_3$, respectively) or less mobility in the cytosol and chloroplasts (Gly-II and Ser-II with pools $C_4$ and $C_5$, respectively). At steady-state photosynthesis, these pools are in diffusional equilibrium with exchange rates $R_3$ and $R_4$, respectively. At the glycine-into-serine conversion step, one molecule of $CO_2$ is released per serine molecule formed, corresponding to a glycine decarboxylation rate of $R_2/4$. The resulting $CO_2$ is re-fixed in the RPPC or the $C_4$ cycle or escapes from the leaf. The extent of re-fixation is described by the re-fixation coefficient $D$, which was experimentally determined as described above.

Formally, the metabolic model is described by the four analytical functions shown as equations 1–4, one for each major metabolite pool (similar to Keerberg *et al.*, 2011). To determine individual pool sizes $C_i$ and carbon fluxes $R_i$, the experimental values of the radioactivity of sugar phosphates, metabolites of the glycine and serine branches of the photorespiratory pathway, and of $C_4$-acids were simultaneously fitted to these functions by multi-component non-linear regression analysis. These functions also consider the time-dependent dilution of the applied tracer $CO_2$ by unlabelled photorespiratory $CO_2$, which is important particularly at the start of tracer feeding under steady-state photosynthesis. A more detailed explanation of these functions is provided in the Supplementary data at *JXB* online.

## Results and discussion

The analysis of *in vivo* Rubisco carboxylation and oxygenation rates is not trivial. Potentially, such data can be extracted from gas exchange experiments (Pärnik and Keerberg, 1995), but this approach is biased by limited knowledge of the internal diffusion pathways for $CO_2$ and $O_2$. Bias becomes even stronger at a varying intercellular distribution of photosynthetic tasks, such as the operation of $CO_2$-concentrating mechanisms. Assuming that there is no large variation in the plastidial $O_2$ concentrations (Tolbert *et al.*, 1995), it should be possible approximately to assess the efficiency of the photorespiratory $CO_2$ pump in $C_3$–$C_4$ intermediate plants by the quantification of carbon fluxes through the individual routes of the photosynthetic–photorespiratory biochemical network. Speed and complexity of the biochemical processes involved require fast and, consequently, sensitive labelling techniques using [14]$CO_2$ as a tracer in combination with model-based data analysis.

For our study, three *Flaveria* species were used, *F. cronquistii* ($C_3$), *F. pubescens* ($C_3$–$C_4$ intermediate), and *F. trinervia* ($C_4$). These species have previously been examined for their photosynthetic types (Apel and Maass, 1981; Ku *et al.*, 1983; Rumpho *et al.*, 1984), kinetic properties of Rubisco (Bauwe, 1984; Wessinger *et al.*, 1989; Kubien *et al.*, 2008), and phylogenetic position within the genus (Powell, 1978; Kopriva *et al.*, 1996; McKown *et al.*, 2005). These studies include the observation (Bassüner *et al.*, 1984; Monson *et al.*, 1986) that $C_3$–$C_4$ intermediate *Flaveria* species fix a small fraction of $CO_2$ via the $C_4$ pathway ($R_6$ in the model shown in Fig. 1) while most of the $CO_2$ enters metabolism directly via the RPPC ($R_1$ in Fig. 1). It was not our intention to perform a comprehensive re-analysis of photosynthetic–photorespiratory carbon

metabolism of these species. Instead, we wanted to focus on the quantification of key fluxes including control data confirming adequate fidelity of our approach.

Building upon previous studies (Pärnik *et al.*, 1987; Keerberg *et al.*, 2011), the model schematically shown in Fig. 1 was developed which embraces, in a generalized form, all the relevant information that is necessary to determine Rubisco carboxylation/oxygenation ratios *in vivo*. It considers time- and flux-dependent changes in the tracer's specific radioactivity at all nodes of the network and allows the separation of high- and low-turnover pools of key metabolites of photosynthetic $CO_2$ and photorespiratory $O_2$ fixation. In order to simplify the model and make it as robust as possible, the metabolically related metabolites of the four major pathways were combined into four pools, each of which is described by a labelling function $P(t,C_i,R_i)$ shown as equations 1–4.

$$P(SP) = S_S \left[ C_1 E_A \left( t, C_1 R_S \right) + C_6 E_I \left( t, C_1, C_6, R_5 \right) \right] \quad (1)$$

$$P(Gly) = S_S \left[ C_2 E_1 \left( t, V_1, C_2, R_2 \right) + C_4 E_1 \left( t, V_2, C_4, R_3 \right) \right] \quad (2)$$

$$P(Ser) = S_S \left[ C_3 E_1 \left( t, V_4, C_3, 0.75 \left( R_2 - R_3 \right) \right) \right. \\ \left. + C_5 E_1 \left( t, V_6, C_5, R_4 \right) + V_6 E_1 \left( t, V_3, V_6, 0.75 R_3 \right) \right] \quad (3)$$

$$P(C_4) = 0.25 S_C C_7 E_A \left( t, 0.25 C_7, R_c \right) \\ + S_S \left[ 0.75 C_7 E_1 \left( t, V_7, 0.75 C_7, R_7 \right) \right. \\ \left. + E_E \left( t, V_8, 0.25 R_8 \right) + E_E \left( t, V_9, 0.75 R_8 \right) \right] \quad (4)$$

Essentially, these four functions describe the time dependence of the radioactivity $P$ incorporated under steady-state conditions into each of the four major model components sugar phosphates plus 3-phosphoglycerate [equation (1); SP-I plus SP-II], the glycine branch [equation (2); Gly-I plus Gly-II] and the serine branch [equation (3); Ser-I plus Ser-II] of the photorespiratory pathway, and the $C_4$ pathway [equation (4); $C_4$]. $S_S$ and $S_C$ are time-dependent functions that describe changes in the specific radioactivity of $CO_2$ fixed in the RPPC and the $C_4$ pathways, respectively. Functions $P(SP)$, $P(Gly)$, $P(Ser)$, and $P(C_4)$ were simultaneously fitted to experimental data points collected over a time scale from 0.6 to 360 s during steady-state photosynthesis. Quantitative values for carbon fluxes $Ri$ between the sub-pools directly involved in photosynthetic $CO_2$ fixation and photorespiration, for example, from SP-I (pool size $C_1$) via Gly-I (pool size $C_2$) to Ser-I (pool size $C_3$), were calculated by multi-component non-linear regression analysis.

Figure 2 demonstrates that the model approximations for all four major metabolite pools represented by the model fit
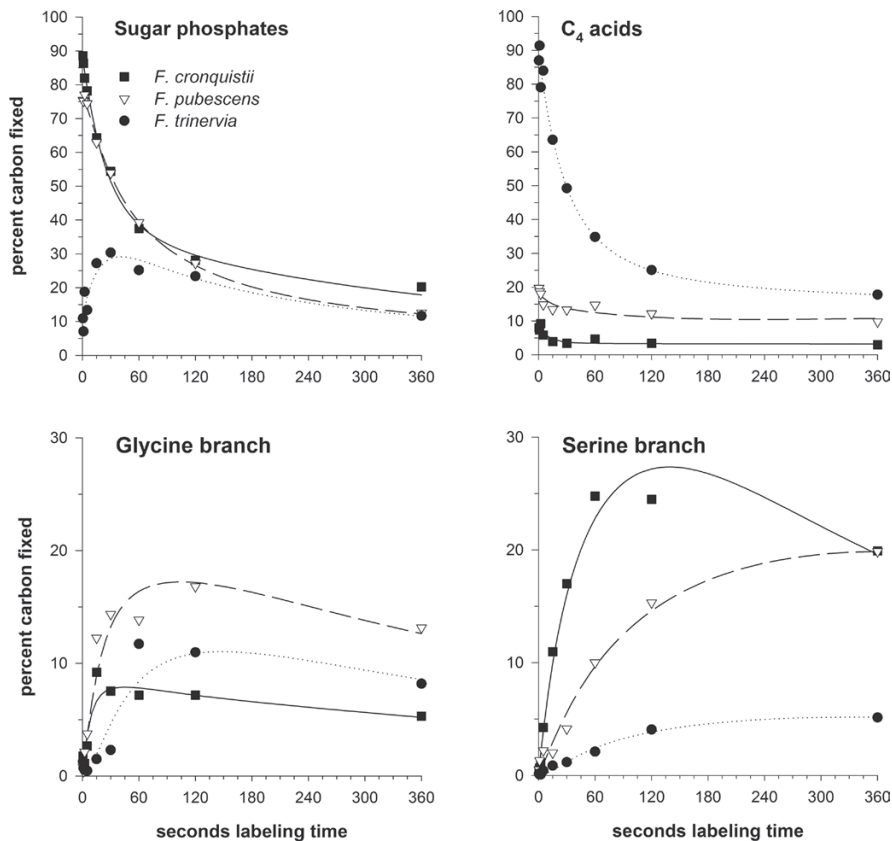


**Fig. 2.** Time-courses of $CO_2$ incorporation into sugar phosphates, $C_4$ acids, and intermediates of the two branches of the photorespiratory pathway. Shown are time-courses relative to true photosynthesis, which was set to 100% for easier comparison. Symbols represent mean values from three data points (biological replicates). Solid (*F. cronquistii*), dashed (*F. pubescens*), and dotted lines (*F. trinervia*) are best fits to the labelling functions (Equations 1–4) and were calculated by multi-component non-linear regression analysis.

very well to the experimental data points. This includes initial $CO_2$ fixation by the $C_4$ pathway in *F. trinervia* in combination with final refixation of $CO_2$ released from $C_4$ acids by the RPPC as well as the 'glycine anomaly' of the $C_3$–$C_4$ intermediate plant *F. pubescens*. As mentioned in the Introduction, the specific alterations to glycine metabolism of $C_3$–$C_4$ intermediate plants are due to a specific distribution of photorespiratory GDC activity (Rawsthorne, 1992), which represents the enzymatic backbone of the photorespiratory $CO_2$ pump.

Another apparent feature is the overlap of primary and secondary labelling kinetics, which is best seen with the $C_4$ acids but also within the glycine and serine branches of the photorespiratory pathway (Keerberg *et al.*, 2011). In the case of the $C_4$ acids, the complex labelling kinetics results from direct $CO_2$ fixation ($R_6$ in Fig. 1), secondary labelling of carbons 1–3 by the synthesis of phosphoenolpyruvate from RPPC intermediates (via phosphoglycerate mutase

and enolase; $R_7$), and export as a metabolically less mobile pool (probably to the vacuole; $R_8$). Also, two metabolic pools with different labelling kinetics exist in both branches of the photorespiratory pathway. This is because one fraction each (Gly-II and Ser-II with pools $C_4$ and $C_5$, respectively) is present in cellular compartments that do not directly contribute to photorespiratory reactions. These fractions show a lower turnover than the photorespiratory most active pools (Gly-I and Ser-I with pools $C_2$ and $C_3$, respectively). At steady-state photosynthesis, the pools equilibrate pairwise with exchange rates $R_3$ and $R_4$. To consider such effects, and specifically calculate fluxes between metabolite pools directly involved in $CO_2$ fixation and photorespiration, the model allows overlapping pools with different labelling kinetics to be separated by component analysis. Figure 3 provides examples of how the sequestration of metabolites into different pools was quantified and how the separation of primary and secondary labelling was achieved in the case of *F. pubescens*. The
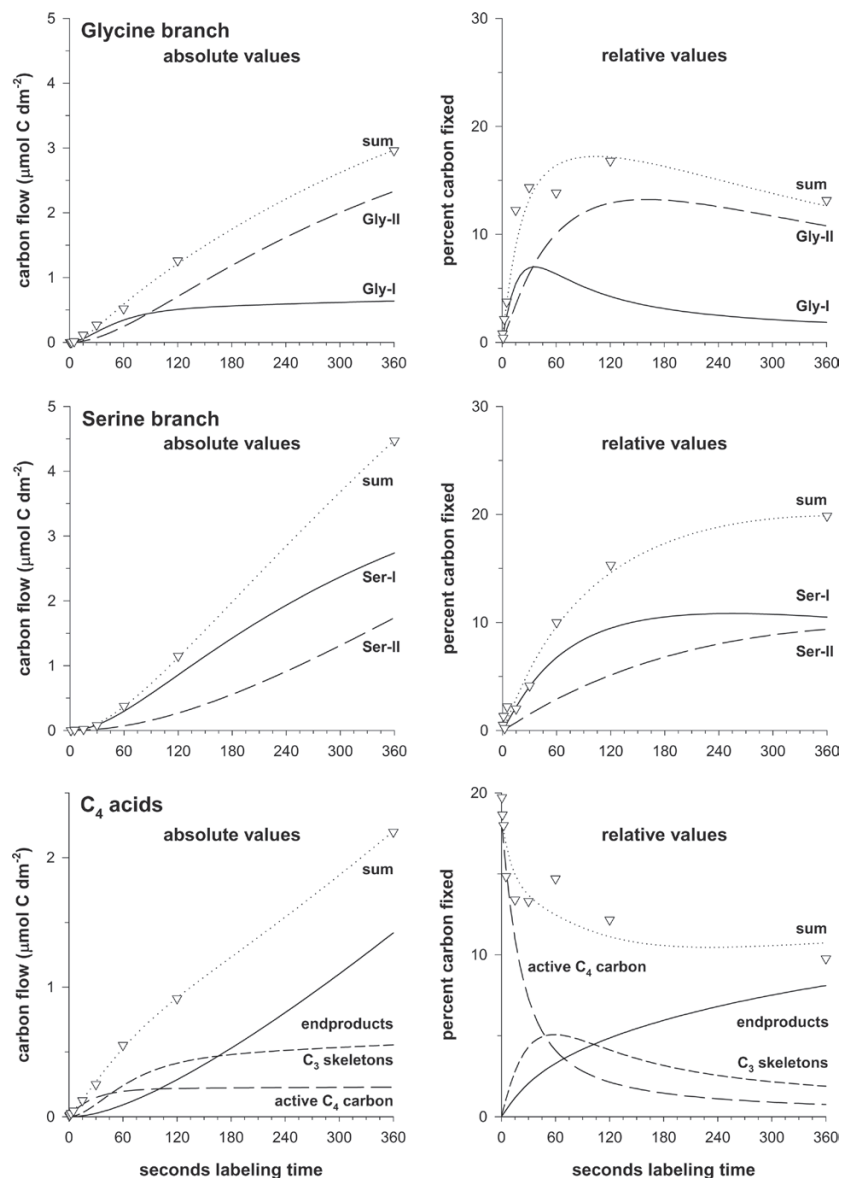


**Fig. 3.** Examples for the model-based separation of fast- and slow-turnover pools in the 'Gly' and 'Ser' branches of the photorespiratory pathway and for primary versus secondary labelling and accumulation of $C_4$ acids. All data are for *F. pubescens*.

example data display carbon incorporation into high- (Gly-I and Ser-I) and low-turnover (Gly-II and Ser-II) pools within the glycine and serine branches of the photorespiratory pathway. They also demonstrate the quantitative separation of the 'active' $C_4$ carbon pool of $C_4$ acids from label appearing in carbon atoms 1–3 and in $C_4$ acids exported to the vacuole. Collectively, these data show that the chosen model is an adequate tool for the calculation of fluxes through the major routes of photosynthetic $CO_2$ fixation from quantitative $^{14}CO_2$ labelling data.

The relevant fluxes are summarized in Table 1 and complemented by results from radiogasometric measurements performed in parallel with the same set of plants. These independent data show rates of true photosynthesis, total decarboxylation, and photorespiratory $CO_2$ evolution. They allowed calculating the extent to which photorespiratory $CO_2$ is re-fixed.

$CO_2$ can become incorporated into the RPPC either directly with rate $R_1$ or indirectly via the $C_4$ pathway with rate $R_6$. The sums $R_1+R_6$ then represent total $CO_2$ incorporation from external sources and show an increasing contribution by the $C_4$ cycle, very low in *F. cronquistii*, low in *F. pubescens*, and, as expected, very high in *F. trinervia*. These total influx rates correspond reasonably well to directly measured rates for true photosynthesis $P_T$, which provides a strong argument for the soundness of all other flux calculations. Higher values for $P_T$ ($C_3<C_3–C_4<C_4$) go together with increased rates of sucrose formation ($R_5$; directly measured in Table 1) and $C_4$ acid accumulation as end-products ($R_8$). Moreover, the photosynthetically active pools of $C_4$ acids ($C_7$; not listed in Table 1) increased from $13\pm1$ ($C_3$) via $57\pm19$ ($C_3–C_4$) to $161\pm39$ µmol C m$^{-2}$ ($C_4$). It is important to note that the increase of $C_4$ cycle activity from *F. cronquistii* to *F. pubescens*

(5.8% to 8.3% of $P_T$, calculated as $R_6–R_8$) is only very small in comparison with the activity of the $C_4$ cycle in *F. trinervia* (81.7% of $P_T$). This suggests that $CO_2$ accumulation occurs mainly by glycine-shuttling and less by $C_4$ cycle activity in the bundle sheath of *F. pubescens*.

Carbon flux through the glycolate cycle, $R_2$, is stoichiometrically related to the rate of RuBP oxygenation, $R_2/2$. As a result of the operation of $CO_2$-concentrating mechanisms in *F. pubescens* and in *F. trinervia*, photorespiration-related fluxes become distinctly lower from $C_3$ towards $C_4$ metabolism. To determine the true rates of RuBP carboxylation, in addition to the sum of $R_1$ and $R_6$, it was necessary to consider the refixation of $CO_2$ generated from internal sources. In $C_3$ and $C_3–C_4$ plants, photorespiration is the dominating internal source of $CO_2$ during photosynthesis. $R_2$ is stoichiometrically related to photorespiratory glycine decarboxylation as $R_2/4$, because one molecule of $CO_2$ is released per one molecule of serine formed from two glycine molecules. The extent to which refixation occurs must be separately determined. This was done by radiogasometric measurements (Pärnik and Keerberg, 1995, 2007), which allowed direct quantification of the sum DEC of photorespiratory glycine decarboxylation plus $C_4$ acid decarboxylation plus minor $CO_2$ releasing processes. It is reasonable to assume that all fractions of internally generated $CO_2$ are re-assimilated with the same efficiency. In combination with the rate $R_P$ of $CO_2$ losses from the leaf (simplifying referred to as photorespiratory $CO_2$ evolution), this assumption allows assessing the partitioning $D$ between re-fixation and loss of $CO_2$ from the leaf. The calculated total rates with which Rubisco fixes $CO_2$ arriving by diffusion from the stomata ($R_1$), from decarboxylation in the $C_4$ cycle ($R_6$), and from photorespiration ($D*R_2/4$) were related to RuBP oxygenation rates ($R_2/2$). The comparison

**Table 1.** *Carbon fluxes in photosynthetic–photorespiratory carbon metabolism of* Flaveria *species*

Values marked with an asterisk represent means ±SE from three measurements on different plants by using a radiogasometric method (Pärnik and Keerberg, 2007). All other values were calculated as means ±SE by multi-component non-linear regression analysis from the time-course of $^{14}C$-incorporation (simultaneous fit to equations 1–4; labelling data from three independent experiments).

| | Carbon fluxes | F. cronquistii µmol m$^{-2}$ s$^{-1}$ | % $P_T$ | F. pubescens µmol m$^{-2}$ s$^{-1}$ | % $P_T$ | F. trinervia µmol m$^{-2}$ s$^{-1}$ | % $P_T$ |
|---|---|---|---|---|---|---|---|
| $P_T$* | True photosynthesis | 3.76±0.10 | | 7.93±0.70 | | 10.37±0.28 | |
| $R_1$ | $CO_2$ incorporation directly into RPPC | 3.82±0.49 | 101.6 | 6.23±0.07 | 78.6 | 0.45±0.25 | 4.3 |
| $R_6$ | $CO_2$ incorporation directly into $C_4$ acids | 0.32±0.01 | 8.5 | 1.29±0.32 | 16.3 | 9.42±0.10 | 90.8 |
| $R_7$ | Secondary labelling of $C_4$ acids $C_1–C_2–C_3$ | 0.43±0.07 | 11.4 | 1.71±0.03 | 21.6 | 1.76±0.21 | 17.0 |
| $R_8$ | $C_4$ acid immobilization as end-products | 0.10±0.01 | 2.7 | 0.66±0.06 | 8.3 | 0.94±0.15 | 9.1 |
| $R_1+R_6$ | Total $CO_2$ incorporation | 4.14±0.49 | 110.1 | 7.52±0.33 | 94.8 | 9.87±0.27 | 95.2 |
| | *of which sucrose formation amounts to | 0.95±0.02 | 25.3 | 2.11±0.09 | 26.6 | 5.98±0.63 | 57.7 |
| | *of which starch formation amounts to | 0.86±0.02 | 22.9 | 1.58±0.13 | 19.9 | 1.80±0.12 | 17.4 |
| | *of which insoluble material amounts to | 0.55±0.02 | 14.6 | 0.75±0.02 | 9.5 | 1.62±0.30 | 15.6 |
| $R_2$ | C flow through photorespiratory pathway | 6.64±0.25 | 176.6 | 3.66±0.20 | 46.2 | 2.56±0.21 | 24.7 |
| $R_2/4$ | Decarboxylation of glycine | 1.66±0.06 | 44.1 | 0.92±0.05 | 11.6 | 0.64±0.05 | 6.2 |
| DEC* | Photorespiratory and $C_4$ decarboxylation | 2.18±0.08 | 58.0 | 1.84±0.05 | 23.2 | 6.70±0.21 | 64.6 |
| $R_P$* | Photorespiratory $CO_2$ evolution | 1.35±0.05 | 35.9 | 0.16±0.02 | 2.0 | 0.03±0.02 | 0.3 |
| $D$* | Reassimilation in % of DEC | | 38.1 | | 91.3 | | 99.5 |
| $R_2/2$ | Oxygenation | 3.3 | | 1.8 | | 1.3 | |
| $R_1+R_6+D*R_2/4$ | Carboxylation | 4.8 | | 8.3 | | 10.5 | |
| | Mean relative $CO_2$ at Rubisco sites | 1.0 | | 3.2 | | 5.7 | |

shows that the resulting *in vivo* carboxylation-to-oxygenation ratio of Rubisco is more than three times higher in *F. pubescens* relative to *F. cronquistii* under the same experimental conditions.

Rubisco from $C_4$ *Flaveria* species has a somewhat lower affinity to $CO_2$, but it is also known that Rubisco from $C_3$ and $C_3$–$C_4$ *Flaveria* species show more or less identical kinetics (Bauwe, 1984; Wessinger *et al.*, 1989; Kubien *et al.*, 2008). Since the oxygen compensation point of $C_3$ plants is only slightly above air levels (Tolbert *et al.*, 1995), plastidial oxygen concentrations are probably close to air oxygen concentrations in *F. cronquistii* and *F. pubescens* but presumably also in the $C_4$ species *F. trinervia*. Therefore, in a comparison of these species, measurement of *in vivo* carboxylation-to-oxygenation ratios allows the calculation of the relative $CO_2$ concentration in chloroplasts. Considering the reported $K_m$ values of Rubisco for $CO_2$, which are even somewhat higher than steady-state internal $CO_2$ levels, our data suggest that the photorespiratory $CO_2$ pump elevates the mean intraplastidial $CO_2$ concentration during steady-state photosynthesis about 3-fold in leaves of the $C_3$–$C_4$ intermediate species *F. pubescens* relative to the $C_3$ species *F. cronquistii*. This is considered to be a sound estimate because small contributions from $C_4$ photosynthesis are balanced by the operation of a significant fraction of Rubisco at non-elevated $CO_2$ levels in the mesophyll of *F. pubescens*.

## Supplementary data

Supplementary data can be found at *JXB* online.

Supplementary data. An explanation of the labelling functions of the model shown in Fig. 1 used for the quantitative analysis of the labelling kinetics.

## Acknowledgements

## References

**Apel P, Maass I.** 1981. Photosynthesis in species of *Flaveria*. $CO_2$ compensation concentration, O2 influence on photosynthetic gas exchange and δ$^{13}$C values in species of *Flaveria* (Asteraceae). *Biochemie und Physiologie der Pflanzen* **176,** 396–399.

**Bassüner B, Keerberg O, Bauwe H, Pärnik T, Keerberg H.** 1984. Photosynthetic $CO_2$ metabolism in $C_3$–$C_4$ intermediate and $C_4$ species of *Flaveria* (Asteraceae). *Biochemie und Physiologie der Pflanzen* **179,** 631–634.

**Bauwe H.** 1984. Photosynthetic enzyme activities and immunofluorescence studies on the localization of ribulose-1,5-*bis*phosphate carboxylase/oxygenase in leaves of $C_3$, $C_4$, and $C_3$–$C_4$ intermediate species of *Flaveria* (Asteraceae). *Biochemie und Physiologie der Pflanzen* **179,** 253–268.

**Bauwe H.** 2011. Photorespiration: the bridge to $C_4$ photosynthesis. In: Raghavendra AS, Sage R, eds. *$C_4$ photosynthesis and related CO_2 concentrating mechanisms*, **Vol. 32**. New York: Springer Science+Business Media BV, 81–108.

**Bauwe H, Keerberg O, Bassüner R, Pärnik T, Bassüner B.** 1987. Reassimilation of carbon dioxide by *Flaveria* (Asteraceae) species representing different types of photosynthesis. *Planta* **172,** 214–218.

**Edwards GE, Ku MSB.** 1987. Biochemistry of $C_3$–$C_4$ intermediates. In: Hatch MD, Boardman NK, eds. *The biochemistry of plants*, **Vol. 10**. London: Academic Press, 275–325.

**Farquhar GD, von Caemmerer S, Berry JA.** 1980. A biochemical model of photosynthetic $CO_2$ assimilation in leaves of $C_3$ species. *Planta* **149,** 78–90.

**Hatch MD, Slack CR.** 1970. Photosynthetic $CO_2$ fixation pathways. *Annual Review of Plant Physiology* **21,** 141–162.

**Holaday AS, Chollet R.** 1983. Photosynthetic/photorespiratory carbon metabolism in the $C_3$–$C_4$ intermediate species, *Moricandia arvensis* and *Panicum milioides*. *Plant Physiology* **73,** 740–745.

**Holaday AS, Chollet R.** 1984. Photosynthetic/photorespiratory characteristics of $C_3$–$C_4$ intermediate species. *Photosynthesis Research* **5,** 307–323.

**Holaday AS, Harrison AT, Chollet R.** 1982. Photosynthetic/photorespiratory $CO_2$ exchange characteristics of the $C_3$–$C_4$ intermediate species, *Moricandia arvensis*. *Plant Science Letters* **27,** 181–189.

**Holaday AS, Lee KW, Chollet R.** 1984. $C_3$–$C_4$ intermediate species in the genus *Flaveria*: leaf anatomy, ultrastructure, and the effect of $O_2$ on the $CO_2$ compensation concentration. *Planta* **160,** 25–32.

**Holbrook GP, Jordan DB, Chollet R.** 1985. Reduced apparent photorespiration by the $C_3$–$C_4$ intermediate species, *Moricandia arvensis* and *Panicum milioides*. *Plant Physiology* **77,** 578–583.

**Hylton CM, Rawsthorne S, Smith AM, Jones DA, Woolhouse HW.** 1988. Glycine decarboxylase is confined to the bundle-sheath cells of leaves of $C_3$–$C_4$ intermediate species. *Planta* **175,** 452–459.

**Keerberg O, Ivanova H, Keerberg H, Pärnik T, Talts P, Gardeström P.** 2011. Quantitative analysis of photosynthetic carbon metabolism in protoplasts and intact leaves of barley. Determination of carbon fluxes and pool sizes of metabolites in different cellular compartments. *BioSystems* **103,** 291–301.

**Kopriva S, Chu CC, Bauwe H.** 1996. Molecular phylogeny of *Flaveria* as deduced from the analysis of nucleotide sequences encoding H-protein of the glycine cleavage system. *Plant, Cell and Environment* **19,** 1028–1036.

**Ku MSB, Monson RK, Littlejohn RO, Nakamoto H, Fisher DB, Edwards GE.** 1983. Photosynthetic characteristics of $C_3$–$C_4$ intermediate *Flaveria* species. I. Leaf anatomy, photosynthetic responses to $O_2$ and $CO_2$, and activities of key enzymes in the $C_3$ and $C_4$ pathways. *Plant Physiology* **71,** 944–948.

**Kubien DS, Whitney SM, Moore PV, Jesson LK.** 2008. The biochemistry of Rubisco in *Flaveria*. *Journal of Experimental Botany* **59,** 1767–1777.

**Laing WA, Ogren WL, Hageman RH.** 1974. Regulation of soybean net photosynthetic $CO_2$ fixation by the interaction of $CO_2$, $O_2$, and ribulose 1,5-diphosphate carboxylase. *Plant Physiology* **54,** 678–685.

**Lüttge U.** 2004. Ecophysiology of Crassulacean Acid Metabolism (CAM). *Annals of Botany* **93,** 629–652.

**McKown AD, Moncalvo JM, Dengler NG.** 2005. Phylogeny of *Flaveria* (Asteraceae) and inference of $C_4$ photosynthesis evolution. *American Journal of Botany* **92,** 1911–1928.

**Monson RK, Edwards GE, Ku MSB.** 1984. $C_3$–$C_4$ intermediate photosynthesis in plants. *BioScience* **34,** 563–574.

**Monson RK, Moore BD, Ku MSB, Edwards GE.** 1986. Co-function of $C_3$- and $C_4$-photosynthetic pathways in $C_3$, $C_4$ and $C_3$–$C_4$ intermediate *Flaveria* species. *Planta* **168,** 493–502.

**Monson RK, Rawsthorne S.** 2000. $C_3$–$C_4$ intermediate photosynthesis. In: Leegood RC, Sharkey TD, von Caemmerer S, eds. *Photosynthesis, physiology and metabolism*, Vol. **9**. Dordrecht: Kluwer Academic Publishers, 553–550.

**Moore BD, Monson RK, Ku MSB, Edwards GE.** 1988. Activities of principal photosynthetic and photorespiratory enzymes in leaf mesophyll and bundle sheath protoplasts from the $C_3$–$C_4$ intermediate *Flaveria ramosissima*. *Plant and Cell Physiology* **29,** 999–1006.

**Ohnishi J, Kanai R.** 1983. Differentiation of photorespiratory activity between mesophyll and bundle sheath cells of $C_4$ plants. I. Glycine oxidation by mitochondria. *Plant and Cell Physiology* **24,** 1411–1420.

**Pärnik T, Keerberg O.** 1995. Decarboxylation of primary and end-products of photosynthesis at different oxygen concentrations. *Journal of Experimental Botany* **46,** 1439–1447.

**Pärnik T, Keerberg O.** 2007. Advanced radiogasometric method for the determination of the rates of photorespiratory and respiratory decarboxylations of primary and stored photosynthates under steady-state photosynthesis. *Physiologia Plantarum* **129,** 34–44.

**Pärnik T, Keerberg OF, Yurisma EY.** 1987. Fast-acting exposure chamber for studying photosynthesis with C-14 $CO_2$. *Soviet Plant Physiology* **34,** 676–683.

**Peisker M.** 1974. A model describing the influence of oxygen on photosynthetic carboxylation. *Photosynthetica* **8,** 47–50.

**Powell AM.** 1978. Systematics of *Flaveria* (Flaveriinae-Asteraceae). *Annals of the Missouri Botanical Garden* **65,** 590–636.

**Rawsthorne S.** 1992. $C_3$–$C_4$ intermediate photosynthesis: linking physiology to gene expression. *The Plant Journal* **2,** 267–274.

**Rumpho ME, Ku MSB, Cheng SH, Edwards GE.** 1984. Photosynthetic characteristics of $C_3$–$C_4$ intermediate *Flaveria* species. III. Reduction of photorespiration by a limited $C_4$ pathway of photosynthesis. *Plant Physiology* **75,** 993–996.

**Sage RF.** 2004. The evolution of $C_4$ photosynthesis. *New Phytologist* **161,** 341–370.

**Sage RF, Sage TL, Kocacinar F.** 2012. Photorespiration and the evolution of $C_4$ photosynthesis. *Annual Review of Plant Biology* **63,** 19–47.

**Schulze S, Mallmann J, Burscheidt J, Koczor M, Streubel M, Bauwe H, Gowik U, Westhoff P.** 2013. Evolution of $C_4$ photosynthesis in the genus *Flaveria*: establishment of a photorespiratory $CO_2$ pump. *The Plant Cell* **25,** 2522–2535.

**Tolbert NE, Benker C, Beck E.** 1995. The oxygen and carbon dioxide compensation points of $C_3$ plants - possible role in regulating atmospheric oxygen. *Proceedings of the National Academy of Sciences, USA* **92,** 11230–11233.

**Värk E, Keerber H, Keerberg O, Pärnik T.** 1968. On the extraction of the products of photosynthesis by ethanol of different concentrations (in Russian). *Proceedings of the Estonian Academy of Sciences (Biology)* **17,** 367–373.

**von Caemmerer S.** 1989. A model of photosynthetic $CO_2$ assimilation and carbon-isotope discrimination in leaves of certain $C_3$–$C_4$ intermediates. *Planta* **178,** 463–474.

**Wessinger ME, Edwards GE, Ku MSB.** 1989. Quantity and kinetic properties of ribulose 1,5-*bis*phosphate carboxylase in $C_3$, $C_4$, and $C_3$–$C_4$ intermediate species of *Flaveria* (Asteraceae). *Plant and Cell Physiology* **30,** 665–671.

**Wiludda C, Schulze S, Gowik U, Engelmann S, Koczor M, Streubel M, Bauwe H, Westhoff P.** 2012. Regulation of the photorespiratory *GLDPA* gene in $C_4$ *Flaveria*: an intricate interplay of transcriptional and posttranscriptional processes. *The Plant Cell* **24,** 137–151.